

True-Color Imagery from GOES—A Synopsis of Past and Present

FREDERICK R. MOSHER and CHRISTOPHER G. HERBSTER
Embry-Riddle Aeronautics University, Daytona Beach, Florida

STEVEN D. MILLER
Cooperative Institute for Research in the Atmosphere, Colorado State University, Fort Collins, Colorado

MIKE ZURANSKI and PAUL SIRVATKA
Meteorology Program, College of DuPage, Glen Ellyn, Illinois

RICHARD A. KOHRS and DAVID HOESE
*Satellite Data Services, Space Science and Engineering Center,
University of Wisconsin-Madison, Madison, Wisconsin*

TIMOTHY J. SCHMIT
*NOAA/NESDIS/Center for Satellite Applications and Research/Advanced Satellite Products Branch,
Madison, Wisconsin*

JAMES P. NELSON
Cooperative Institute for Meteorological Satellite Studies, University of Wisconsin–Madison, Madison, Wisconsin

ROBERT HALEY
NOAA, National Weather Service, Melbourne, Florida

(Manuscript received 15 March 2022; review completed 23 November 2022)

ABSTRACT

The human eye is sensitive to three primary bands of light—centered on the red, green, and blue parts of the visible spectrum. The human eye is not very sensitive to variations in shades of gray—being able to distinguish only approximately 25 different gradations of gray in satellite images. However, by using the three different color sensors, the eye has the potential to distinguish up to a million different values of color. Hence, color is a powerful tool for distinguishing various objects of interest with subtle intensity variations.

The *Geostationary Operational Environmental Satellites-R (GOES-R)* series of geostationary satellites do not have a green channel. However, a synthetic green channel can be constructed from the blue, red, and near-infrared “veggie” channels for the use in a true-color visible image. Since the launch of the *GOES-16* satellite, several different groups have developed color visible algorithms that are available on public websites. The purpose of this paper is to help explain the similarities and differences of true-color *GOES* images that are on the web and in other locations.

1. Introduction

The human eye has three different types of light sensitive cone cells enabling daytime color vision. The red cone cells respond to light with a peak sensitivity around 564–580 nm; the green cone cells have a peak

sensitivity around 534–555 nm; and the blue cones have a peak sensitivity around 420–440 nm (Hunt 2004). The brain processes the signals from these three types of cones to interpret the color of an object. If the signal from the long-wavelength cone cells is greater than the other two types, the brain perceives the object

as red. If the signals from the red and green cones are stronger than from the blue, the brain perceives the object as yellow. Figure 1 shows the spectral response of the three types of cone cells.

The *Geostationary Operational Environmental Satellites (GOES)* generates images with 4096 shades of brightness, except for channel 7 ($3.9\mu\text{m}$) that has 16 384 shades (Schmit et al. 2017). The human eye cannot see that many shades. Studies (e.g., Corbell et al. 1976) show that one can distinguish only around 25 gray shades in a satellite image. If one uses rigid geometric patterns, the number of discernible gray shades increases to around 100 shades. Because the human eye has the three types of cone cells, the number of perceived color shades increases to the cube of the perceived gray shades. This allows one to see many thousands ($25^3 = 15\,625$) to more than a million ($100^3 = 1\,000\,000$) color shades. Hence, color is a powerful tool for distinguishing various objects of interest with subtle intensity variations using three separate gray-scale images combined into a red, green, blue (RGB) display.

2. History of transition of black and white to true-color geostationary satellite images

When photography first became available in the mid-1800s, the technology for recording images was monochrome with black and white images. Most movies and home photography were produced in black and white through the 1950s. By the 1960s the price of color film became comparable to black and white film, and by the 1970s most movies and photography had adopted color. The 1973 hit song *Kodachrome* by Paul Simon captured the mood of the time with the words “everything looks worse in black and white.” Television also started out with black and white displays. Whereas the National Television System Committee color broadcast standard was adopted in 1953, very few color television broadcasts were available until the mid-1960s when there was a rapid conversion of broadcasts to color. Between 1964 and 1967, all the television network broadcasts were converted to color (https://en.wikipedia.org/wiki/Color_television).

Likewise, the first weather satellite images were black and white. The first geostationary satellite, the Applications Technology Satellite (ATS-1), carried an experimental spin scan cloud camera developed by V. Suomi and R. Parent of the University of Wisconsin-Madison. NASA’s ATS-1 was launched on 7 December

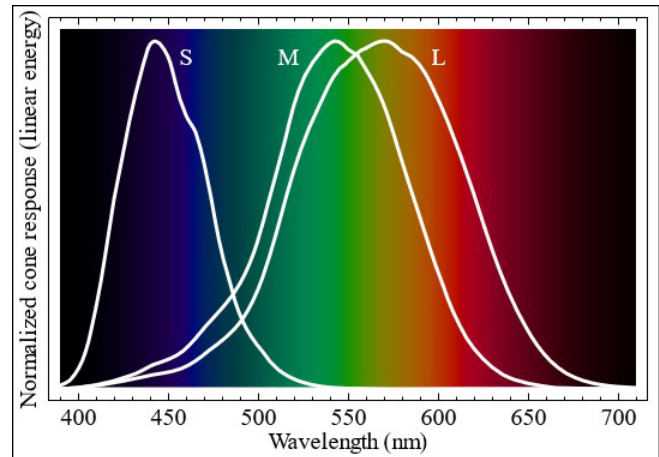


Figure 1. Spectral response of the three types of cone cells in the human eye. The SML letters refer to short, medium, and long wavelengths. Image courtesy of https://en.wikipedia.org/wiki/Cone_cell. Click image for an external version; this applies to all figures hereafter.

1966, and by 11 December, the satellite generated images of the Earth over the Pacific Ocean every 30 min. The images had 13 gray shades and were featured on the cover of the February 1967 *Bulletin of the American Meteorological Society* (McQuain 1967).

The success of the ATS-1 led to the development of a second-generation instrument. Consistent with the trends in the 1960s of conversion of black and white to color, the next geostationary satellite ATS-3 carried the Multicolor Spin-Scan Cloud Camera. The ATS-3 was launched 5 November 1967 and started taking color images of the Earth on 10 November 1967. The first color images were featured on the February 1968 issue of the *Bulletin of the American Meteorological Society* (Suomi and Parent 1968). Users of the ATS-3 color images commented that “The superiority over monochrome pictures (black and white) is demonstrated by the strikingly better contrast between clouds and the background (Earth surface)” (Warnecke and Sunderlin 1968). The color images were generated every 30 min for the next three months, when the red and blue channels failed. The remaining channel was used for black and white images for the next six years.

One of the greatest limitations of the conventional visible band is that it is available only during daylight. Hence, when the first operational geostationary weather satellite was designed, an infrared channel accompanied the single visible channel. The infrared channel measures the temperature of the clouds (and

surfaces) and is available both day and night. For the next 40 years, a variety of infrared channels were added to the geostationary weather satellites of the world, but the visible channel was limited to a single band in the red region of the spectrum. During these 40 years, satellite hardware has evolved through several generations of technology.

In the late 1990s planning started for the next generation of the United States *GOES*. The planning started with a series of meetings with the scientific community to determine the sensor requirements for the Advanced Baseline Imager (ABI; Davis 2001). The rules for channel selection dictated by the National Oceanic and Atmospheric Administration (NOAA) included that the channel could be used to generate a scientific product useful for weather forecasting, and that previous experience with the proposed channel on other satellite systems had demonstrated the feasibility of success for the proposed channel. The red channel easily won approval based on past performance, having been included on every weather satellite since *GOES-1*. A blue channel also won approval, as it can be used to detect slant range visibility for aviation, detect smoke and haze, provide inputs to air pollution studies, and provide inputs for clear-sky radiance calculations (Schmit et al. 2005). The request for a “veggie” channel in the near infrared also gained approval. Polar-orbiting weather satellites had already included this channel for many years, which was used to generate a normalized difference vegetation index—showing active vegetation areas (Tucker 1979).

Despite the successful inclusion of these additional visible-spectrum bands, the request for a green channel ran into problems. The primary reason stated for wanting a green channel was to generate true-color satellite images (Davis 2004). NOAA management argued that color images had aesthetic value rather than scientific usefulness. Supporters of the true-color images argued that it would differentiate between clouds and smoke, volcanic ash, and dust suspended in the air—helping forecasters make better use of ABI imagery for situational awareness. Management countered that other approved channels could be used to generate products depicting these hazards, and there was no “validated, user requirement” for true-color imagery. In the end, the NOAA decision was that the aesthetic value of color images was not worth the additional investment that would be required to include a green channel. The ABI channels selected for the

GOES-R, and the rationale for each, are described in Schmit et al. (2005).

During the 10+ years between the final selection of the ABI channels and the launch of the *GOES-R* satellite, several groups were funded to develop processing algorithms for the new *GOES* data (Goodman et al. 2012). A total of 25 algorithms were developed for day-one implementation, and another 32 algorithms were specified for eventual development. These were mostly a subset of products requested by the National Weather Service (NWS). These algorithms did not include any true-color visible images.

However, the dream of true-color geostationary images lived on among research teams who were integrated with operational users and perceived the value of this capability. Researchers at the Cooperative Institute for Research in the Atmosphere (CIRA) at Colorado State University (CSU) and the Cooperative Institute for Meteorological Satellite Studies (CIMSS) at the University of Wisconsin-Madison published a paper (Miller et al. 2012) that described a method of how to generate a synthetic green channel on the *GOES-R* using the approved blue, red, and veggie channels. The feasibility of the method was demonstrated using polar-orbiting satellite data [the Moderate Resolution Imaging Spectroradiometer (MODIS)]. A later paper discussed a similar method to generate a synthetic green spectral band (Bah et al. 2018).

The utility of the synthetic green channel would be demonstrated with the launch of the Japanese Himawari-8 (Japanese for sunflower) satellite on 7 October 2014, almost two years prior to the launch of the *GOES-R* satellite. To improve the appearance of the Himawari-8 images, Miller et al. (2016) blended the Himawari-8 veggie channel with the original green channel to generate a hybrid green channel for the visible color images. The Miller et al. (2016) paper made the front cover of the October 2016 issue of the Bulletin of the American Meteorological Society, just as the *GOES-R* satellite was launched on 19 November 2016 and became *GOES-16*.

The first month after the launch of *GOES-16* was devoted to instrument checkout. During this time NOAA started preparing a *GOES-16* press release timed to coincide with the January annual meeting of the American Meteorological Society (AMS). The NOAA Office of Communications contacted the imagery team and asked for a true-color visible image from the new *GOES-16*. Because true-color visible was

not one of the official products, and the ABI did not include a native green band, the imagery team developed a synthetic green channel using the Miller et al. (2012, 2016) technique. By the first day of the AMS meeting NOAA released a true-color image to showcase the first *GOES-16* ABI image, shown in Fig. 2.

The next 10 months after the first image release were devoted to the scientific checkout of the satellite. The *GOES-16* data processing was a challenge to organizations generating satellite displays for users. The number of available channels increased from five on the *GOES-15* to 16 on the *GOES-16* (Schmit et al. 2017, 2018). The resolution of the sensors doubled, generating four times as much data for each channel. The frequency of scans increased from 15 (or 30) min for the contiguous United States (CONUS) to 5 min. The hemispheric scan frequency increased from 30 min to 15 (and eventually to 10 min). Plus, there were two meso-sectors with a cadence of 1 min.

While some satellite websites maintained the traditional visible, infrared, and water-vapor image selections, other websites embraced the potential for new satellite products utilizing *GOES-16* data. The remainder of this article considers five website providers of true-color imagery and other satellite imagery products: (i) the Space Science and Engineering Center (SSEC), University of Wisconsin-Madison at <https://www.ssec.wisc.edu/data/geo/>, (ii) SSEC at <https://geosphere.ssec.wisc.edu/>, (iii) the College of DuPage (COD) at <https://weather.cod.edu/satrad/>, (iv) the Embry-Riddle Aeronautical University (ERAU) at https://wx.erau.edu/erau_sat/, and (v) CIRA (<https://rammb-slider.cira.colostate.edu>), whose true-color application (presented as GeoColor; Miller et al. 2020) also is hosted by NOAA at <https://www.star.nesdis.noaa.gov/GOES/>. Because there is no official algorithm for the generation of true-color visible images, each of the five providers developed their own algorithm. While there are similarities in the true-color visible products, there also are noticeable differences. The following is a description of each of the true-color imagery sources and how each of the organizations generate a true-color visible product.

3. Rendering a synthetic green channel to enable true color from ABI

Because the current *GOES* satellites do not have a green channel, a synthetic green channel is required for

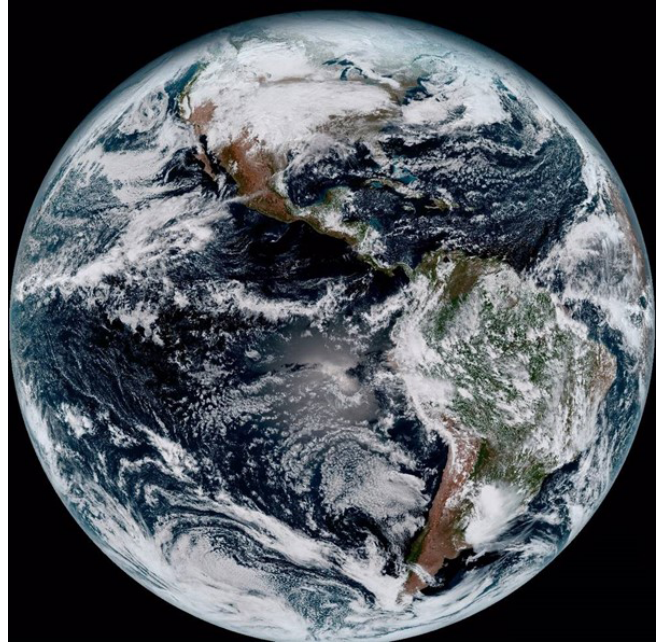


Figure 2. The first image from *GOES-16*, taken at 1:07 pm EST 15 January 2017, was in color, even though the approved *GOES* processing algorithms did not include a visible color algorithm. It was created using channels 1, 2, and 3 of the 16 spectral channels available on the satellite's sophisticated Advanced Baseline Imager (ABI).

the display of true-color images. Figure 3 [adapted from Fig. 4 in Schmit et al. (2018)] shows the relative reflectance for grass (green line) and snow (blue line) over the visible and near-infrared spectrum and the placement of the ABI channels 1–5. Channel 1 is the blue channel. The relative peak of about 10% in the grass reflectance between channels 1 and 2 is the green grass signature seen by human eyes. Channel 3 is the veggie channel, which shows a relatively large reflectance of about 50% of sunlight by grass. The reflectance of snow and clouds is fairly uniform for channels 1–3. Hence, to generate a “green” channel from the veggie channel, one must reduce the brightness of the pixels containing vegetation such as grass or tree leaves, while not impacting the pixels containing clouds or snow.

Miller et al. (2012) outlined a statistical approach used to generate a “synthetic green” channel that has been utilized for the CIRA/NOAA processing. The approach involves enlisting an observing system (polar satellite MODIS data) with blue, green, red, and near-infrared (865 nm) veggie channels. All bands are Rayleigh corrected as a preprocessing step to remove

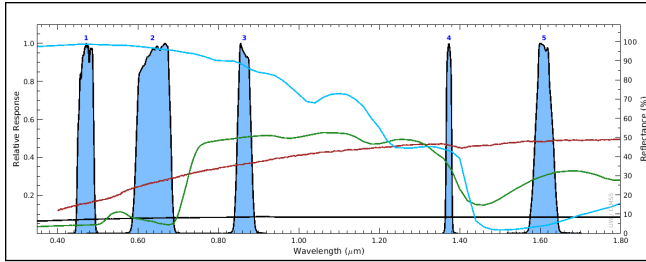


Figure 3. Relative reflectance for grass (green line), snow (blue line), dirt (brown line), and asphalt (black line) over the visible and near-infrared spectrum and the placement of the spectral response functions of the ABI channels 1–5. Image adapted from Fig. 4 in Schmit et al. (2018).

molecular scatter, which sharpens the detail. A look-up table of green as a function of the other three Rayleigh-corrected bands was formulated and stratified according to the surface type. The stratification of the look-up table accounts for the fact that green tonality can arise from both chlorophyll-a reflectance as well as from color mixing (e.g., in shallow waters with sandy bottoms, such as the Bahama shoals). The green members of a blue/green/red triplet are averaged to provide an indexed value. The CIRA technique yields a high-quality version of true-color imagery that has been adopted by NOAA/National Environmental Satellite, Data, and Information Service (NESDIS).

The SSEC, ERAU, and COD approach is to do an empirically derived weighted average of channels 1, 2, and 3. The pixels containing clouds and snow will have similar brightness in all three channels, so the average will retain the brightness of the clouds. The pixels with vegetation will have lower brightness values in channels 1 (C1) and 2 (C2), so the channel 3 (C3) brightness will be reduced with the weighted average. The SSEC and COD true-color products use weights of $0.45(C2) + 0.10(C3) + 0.45(C1)$. The SSEC GeoSphere uses weights of $0.465(C2) + 0.07(C3) + 0.465(C1)$. The ERAU day/night visible product uses weights of $0.40(C2) + 0.20(C3) + 0.36(C1)$. Channel 3 cloud images are slightly brighter than channel 1 and 2, so the 0.96 sum allows for the green channel clouds to be the same brightness as the other channels, making white clouds. Figure 4 shows a black/white channel 2 image, while Figs. 5 through 9 show each of the provider's version of the true-color image.

The different providers of color visible images utilize different weights in the generation of the green channel and have different results. Which one is

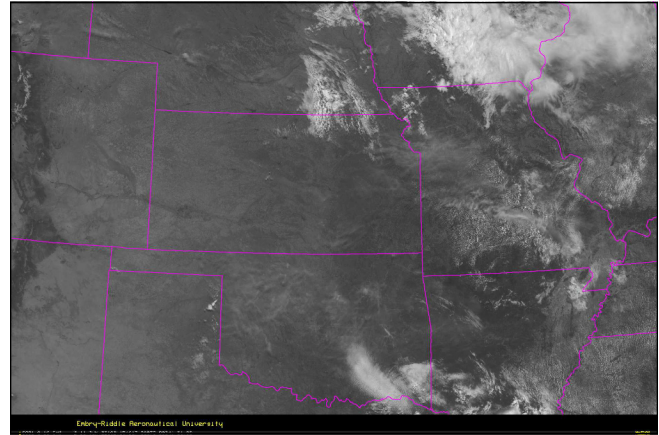


Figure 4. ERAU black/white visible channel 2 image for the central Midwest at 1546 UTC 11 June 2022.

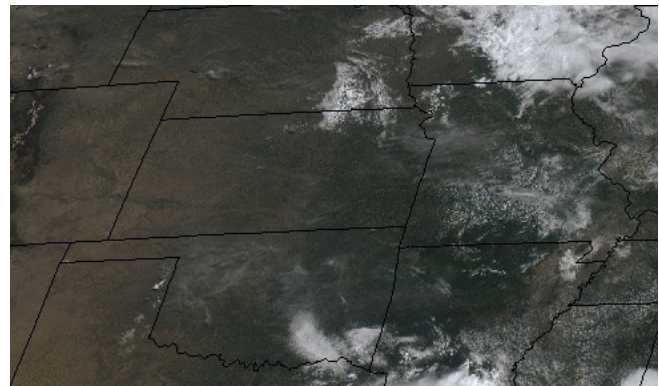


Figure 5. SSEC true-color image for the same time as in Fig. 4. The SSEC true-color image uses weights of $0.45(C2) + 0.10(C3) + 0.45(C1)$ to generate the green channel.

correct? Probably none of them. The reflectance by plants and other surfaces has been studied extensively by the remote-sensing community. The ratio of the peak in the 0.55- μm green band to the peak in the 0.8- μm veggie band varies with the type of plant, and with the stress that the plant is under. The ratios for different plant studies range from 0.37 to 0.09. Most *GOES* ABI visible band pixels most likely contain different plants reflecting differently in the two wavelengths. Hence, the synthetic green channel will not be accurate for all situations. Only a green channel on future geostationary satellites would provide actual green reflectance. With that said, the primary objective of true-color visible imagery is to provide a qualitative approximation to color vision that enables users to interpret the complex environmental scene from a baseline of familiarity. Each of the true-color generation algorithms

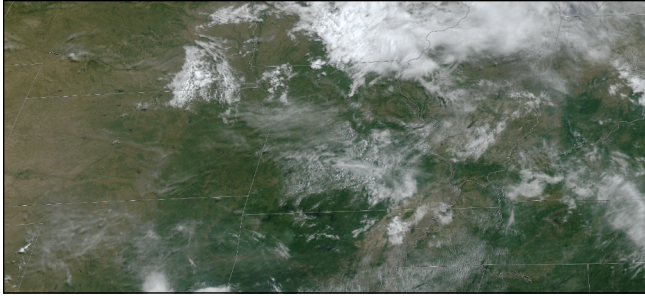


Figure 6. SSEC GeoSphere image for the same time as in Fig. 4. The SSEC GeoSphere image uses weights of $0.465(C2) + 0.07(C3) + 0.465(C1)$ to generate the green channel. The image extends slightly further east as compared to Fig. 4.

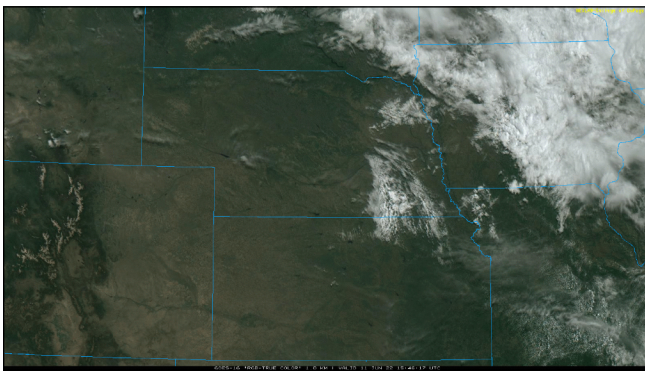


Figure 7. COD true-color image for the same time and approximate location as in Fig. 4. The COD true-color image uses weights of $0.45(C2) + 0.10(C3) + 0.45(C1)$ to generate the green channel.

highlighted in this paper fulfill these scene interpretation objectives.

One advantage of the true-color images is the discrimination of dim clouds. The Fig. 9 animation is a “Wizard of Oz” loop with the first half being black/white channel 2 images and the second half being the true-color product of CIRA/NESDIS. Dim cirrus clouds over Oklahoma and the dim small clouds from southern Missouri to northern Mississippi are easier to see in the true-color product as compared to the traditional black/white visible. Another advantage of the true color is to provide discrimination of meteorological clouds from aerosol clouds of volcanic ash, dust storms, and biomass smoke plumes. The CIRA/NOAA true-color image at 2144 UTC 29 April 2022 (Fig. 10) shows smoke coming from forest fires in New Mexico, a dust storm coming from southern Colorado, and meteorological clouds and mountain snow. The Fig. 10 animation shows a 2.5-h sequence of

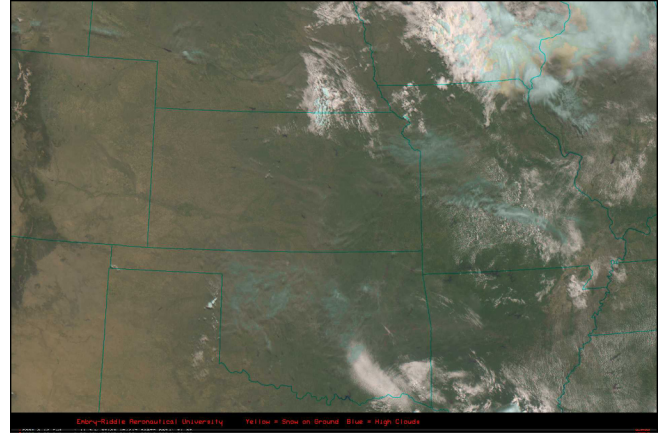


Figure 8. ERAU day/night visible image for the same time as in Fig. 4. The ERAU day/night visible image uses weights of $0.40(C2) + 0.20(C3) + 0.36(C1)$ to generate the green channel.

the CIRA/NOAA true-color images utilizing the meso-sector 1-min images. The dust is brown, the smoke is blue/gray, and the clouds are white.

4. Space Science and Engineering Center (SSEC) images

The success of the ATS-1 and ATS-3 satellites led V. Suomi to establish the SSEC as a research and development institute within the University of Wisconsin-Madison. For the past 50 years, SSEC has been a world leader in the development of new weather satellite technology, satellite data access, satellite and weather data processing, and weather satellite data utilization. Co-located with SSEC is the NOAA-supported CIMSS. SSEC developed and still supports the Man Computer Interactive Data Access System (McIDAS) software package (Suomi et al. 1983), which is utilized by many weather satellite data providers, including COD, ERAU, and CIRA/NOAA; this will be discussed in subsequent sections.

The generic website at <https://www.ssec.wisc.edu> has a variety of links, of which the <https://www.ssec.wisc.edu/data/geo> website is the one of most interest for this section. This website offers access to all the weather geostationary satellites around the world. For *GOES-16* and *GOES-18* (*GOES-EAST* and *GOES-WEST*), the website offers displays of any of the 16 channels, as well as a visible true-color display. The true-color image is a RGB combination of the red, synthetic green, and blue channels of the original satellite data. The images are displayed in the native

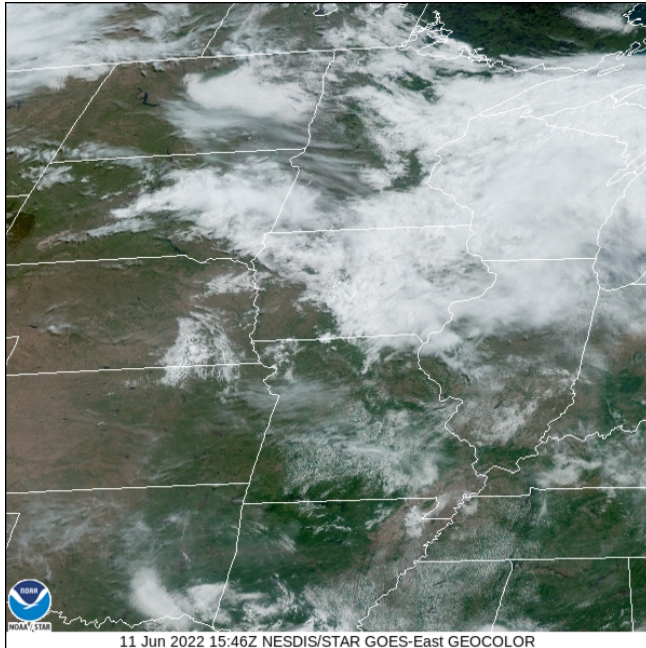


Figure 9. CIRA/NOAA true-color product for the same time as in Fig. 4. The CIRA/NOAA product uses a statistical approach to generate a “synthetic green” channel. The statistical approach relates the polar satellite MODIS data with blue, green, red, and near-infrared (865 nm) veggie channels to a synthetic green channel generated from red, blue, and veggie data. [Click on image for animation.] The animation is a “Wizard of Oz” loop with the first half being black/white channel 2 images and the second half being the true-color product of CIRA/NESDIS. Dim cirrus clouds over OK and the dim small clouds from southern MO to northern MS are easier to see in the true-color product as compared to the traditional black/white visible images.

GOES satellite projection, with the original observed band brightness. Hence during nighttime, the true-color images are black. The website also has a *GOES-16* RGB/infrared satellite selection that offers full-disk imagery, and a Wisconsin sector that inserts the infrared image into the true-color image where it is night. However, the CONUS scans are not offered in this format.

The *GOES* displays are available as 10-min full-disk, 5-min CONUS, and two 1-min meso-sector floater regions. The animations are offered with a range of 1–152 images in a loop. Figure 11 shows the SSEC true-color image for the *GOES-16* CONUS scan at 1251 UTC 14 May 2021. The West Coast of the United States is still in darkness. An important advantage of this

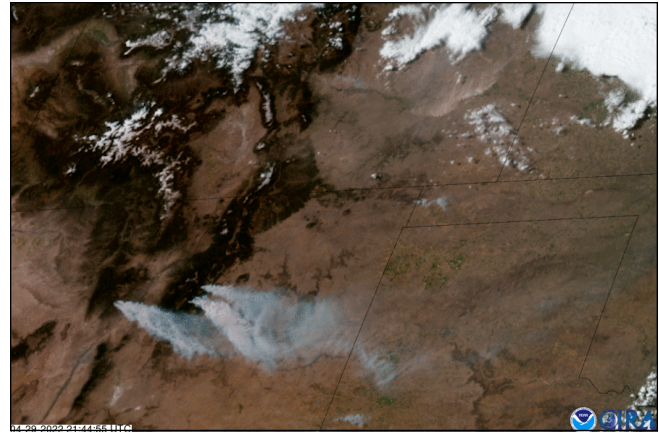


Figure 10. CIRA/NOAA true-color image at 2144 UTC 29 April 2022 showing smoke coming from forest fires in NM and a dust storm coming from southern CO—along with meteorological clouds and mountain snow. The dust is brown, the smoke is blue-gray, and the clouds are white. [Click on image for animation.] The animation shows a 2.5-h sequence of the CIRA/NOAA true-color images utilizing the meso-sector 1-min images.

technique over others is its portability; the technique is readily integrated into most display systems, including the Advanced Weather Interactive Processing System (AWIPS) workstations used by operational NOAA forecasters.

5. SSEC CSPP GeoSphere

Recently, the SSEC released a Python-based software package and website for the Community Satellite Processing Package (CSPP) for Geostationary (Geo) Data. A more detailed description of the free software is available at <http://cimss.ssec.wisc.edu/cspgeo>. The look and feel of the CSPP GeoSphere data (<https://geosphere.ssec.wisc.edu>) are very different from that of the other true-color websites discussed in this paper. The current *GOES* satellites generate an image by first electronically scanning an array of sensors to generate a tile of data. *GOES* then mechanically moves the array to the next location to be scanned. The CSPP GeoSphere utilizes the original tiles for the displays, while the other websites using the McIDAS software utilize a preprocessor ingestor that combines all the individual tiles into a continuous “Area” file for each channel.

The CSPP GeoSphere image processing first generates daytime Rayleigh-corrected images for

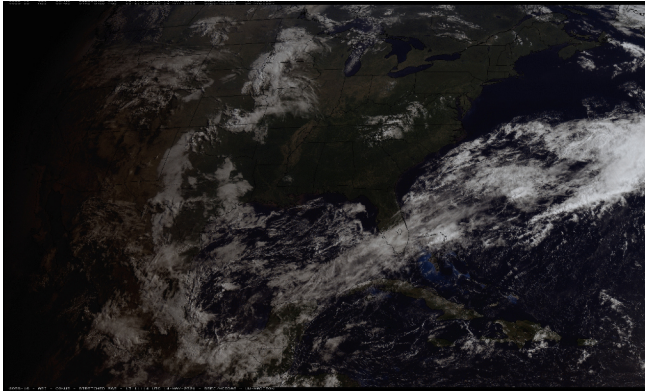


Figure 11. SSEC true-color GOES-16 CONUS image at 1251 UTC 14 May 2021. The West Coast of the United States is still in the dark. The RGB image is constructed from the GOES-16 blue channel 1, red channel 2, and a synthetic green channel constructed from channels 1, 2 and 3. [Click on image for animation.]

channels 1 (blue), 2 (red), and 3 (veggie) as suggested by Miller et al. (2012). The images also are brightness normalized. The brightness of an image changes during the day because of changes in the solar zenith angle (the angle between a line perpendicular to the Earth at a given location and a line pointing toward the sun). If all surfaces scattered light equally in all directions (isotropic scattering) the brightness of a given scene would be a constant multiplied by the cosine of the solar zenith angle. A first order brightness normalization is to divide the observed brightness of a pixel by the cosine of the solar zenith angle. The synthetic green image is generated as described in section 3. The nighttime portions of the image are populated with a nighttime microphysics image (https://rammb.cira.colostate.edu/training/visit/quick_guides/QuickGuide_GOESR_NtMicroRGB_Final_20191206.pdf). The daytime and nighttime RGB images are blended over an approximate 3° band (two pictures) at the terminator zone. Figure 12 shows the CSPP GeoSphere CONUS display for 1251 UTC 14 May 2021 (the same time as in Fig. 11). Figure 13 shows nighttime low clouds over Texas at 0926 UTC 11 June 2022. The low clouds are cyan colored.

6. College of DuPage (COD) true-color images

COD is a community college located outside Chicago, Illinois. It is the second largest provider of undergraduate education in the state of Illinois. It offers

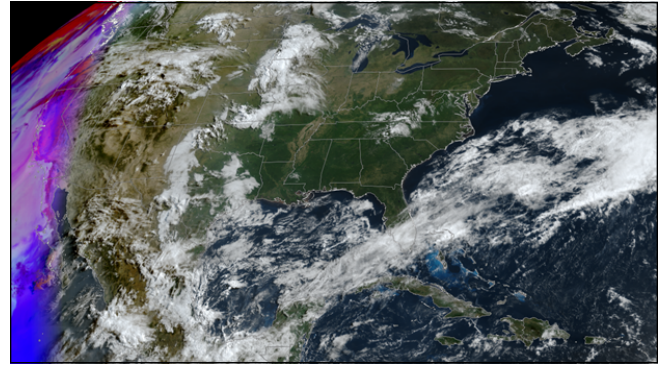


Figure 12. CSPP GeoSphere image at 1251 UTC 14 May 2021 (the same time as in Fig. 11). The RGB channels have been corrected for Rayleigh scattering and sun-angle changes. The nighttime portions of the image are the nighttime microphysics image with red being high ice clouds. [Click on image for animation.]

an extensive weather website (<https://weather.cod.edu>), and for satellite data (<https://weather.cod.edu/satrad>) offers *GOES-East* and *GOES-West* displays for the 16 ABI channels, a true-color visible product, plus seven other RGB-derived products. All the products are available for full-disk, CONUS, and various sector displays. For *GOES-East* there are 11 global sectors, five continental sectors, 16 regional sectors, 53 sub-regional sectors, and 111 localized sectors, all of which auto-refresh.

In addition to the generation of the synthetic green channel, the COD product uses several image processing tools to make the resultant imagery easier to interpret. The first is image remapping. The satellite scanning of the 3-dimensional Earth into a 2-dimensional image results in distortions. Remapping this native satellite projection imagery into a commonly used map projection can make the imagery easier to interpret, especially near the Earth's edge. The remapping software available in the McIDAS system (Suomi et al. 1983) allows one to specify a map projection, resolution, size, and center point of the desired remapped image. The COD image processing remaps the midlatitude regions into Lambert Conformal projections, tropical scans into Mercator projections, and polar regions into Polar Stereographic projections. The subsector datasets are then sectorized from the regional basic remap without further remapping.

COD visible images are brightness normalized as specified in Eq. (1), which can add almost an hour of usable visible imagery after sunrise and before sunset.

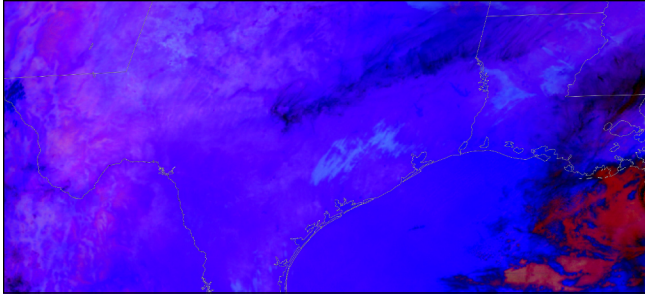


Figure 13. CSPP nighttime clouds at 0926 UTC 11 June 2022 along the TX coast. The low clouds are a cyan blue color. [Click on image for animation.]

$$I = \sqrt{I_o^2 / (\cos \theta * corr)} \quad (1)$$

For visible satellite images, NOAA applies a square root digitization to the albedo of the observed brightness. This expands the dynamic range of the displayed brightness, allowing for the user to see both clouds and ground in the same image. In Eq. (1), I_o is the original pixel brightness and I is the normalized brightness. The image pixel brightness is squared to bring it back to the original albedo and then divided by the cosine of the solar zenith angle, θ , which is the angle between the vertical line at the point of observation and the line pointing toward the sun. The spherical shape of the Earth causes the incoming energy from the sun to be spread out as a function of the incoming energy times $\cos(\theta)$. Dividing by $\cos(\theta)$ normalizes the brightness to what a flat Earth would receive. The term *corr* is an empirically derived correction function developed at ERAU to correct for forward light scatter by clouds. The *corr* term was developed from the observed brightness of trade wind cumulus clouds for a variety of sun/satellite angles and expressed as a function of the scattering angle between the line pointing to the sun and the line pointing to the satellite. The resultant function has values of 1 for scattering angles between 0 and 100°. The function then increases linearly to 2.2 at 140°, to 3.7 at 165°, and finally to 8.95 at 180°. The correction function has little impact except for sunrise on the *GOES* eastern horizon and sunset on the *GOES* western horizon. Finally, the square root then brings it all back to the NOAA digitization scale.

For COD true-color images, channel 7 black and white infrared remapped imagery is inserted into the nighttime portions of the image. As a result, a user of true-color imagery during the day can still use the

satellite information for decisions after dark. Figure 14 shows the resultant COD true-color image at 1251 UTC 14 May 2021, which is the same time as the SSEC products shown in Figs. 11 and 12. Figure 15 shows COD nighttime low clouds over Texas at 0926 UTC 11 June 2022. The low clouds are close to the temperature of the ground, so they are hard to see.

7. Embry-Riddle Aeronautical University–Daytona Beach (ERAU) Day/Night visible images

ERAU is a private, nonprofit university in Daytona Beach, Florida, that specializes in aviation-related degree programs, including meteorology and aeronautical science degrees. The ERAU satellite data website (http://wx.erau.edu/erau_sat) offers *GOES-East* and *GOES-West* displays of day/night visible color images, as well as other derived satellite products. The *GOES-East* displays are available for the entire hemisphere, 16 regional hemispheric sectors, the entire CONUS, six regional displays, 21 localized sectors, and the two 1-min mesoscale sectors. The *GOES-West* displays include the full hemisphere, 13 regional sectors, the entire western United States to Hawaii and up to Alaska, nine localized sectors, and the two 1-min mesoscale sectors, all of which auto-refresh.

Like COD, ERAU also remaps the satellite images into standard map projections. ERAU remaps each sector into its own desired projection. For the polar regions, a Polar Stereographic projection is generally used. For the midlatitudes, a Lambert Conformal projection is used. And for the tropical and full-disk images, a rectilinear projection (equal map distances for equal latitudes and longitudes) is used.

ERAU also performs brightness normalization like COD using Eq. (1). Miller et. al. (2016) has shown that if the Rayleigh scattering is removed, the resultant color image looks crisper and cleaner. As part of the brightness normalization for the blue channel, an empirical Rayleigh scattering correction has been added to Eq. (1).

$$I = \sqrt{\frac{I_o^2}{(\cos \theta * corr)} - 3280 * (1 + 1.3 \sin \theta \sin \phi)} \quad (2)$$

The $\sin \theta \sin \phi$ term in Eq. (2) multiplies the sines of the solar zenith angle and the satellite zenith angle. The correction coefficient was empirically developed using

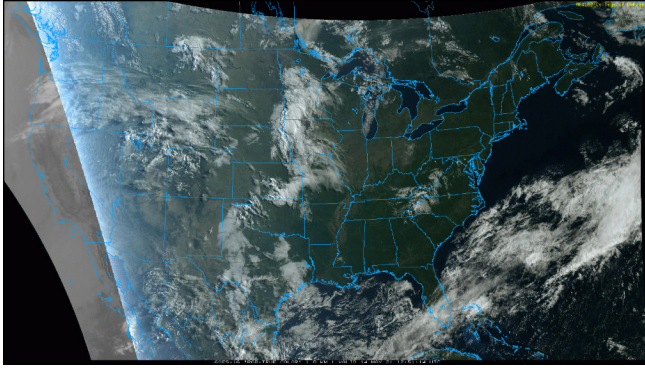


Figure 14. COD true-color image at 1251 UTC 14 May 2021 (the same time as in Figs. 11 and 12). The three channels have been remapped into a Lambert Conformal projection to allow for better viewing near the earth edge, have been brightness-normalized, and infrared imagery has been inserted into the dark portions of the true-color image. [[Click on image for animation.](#)]

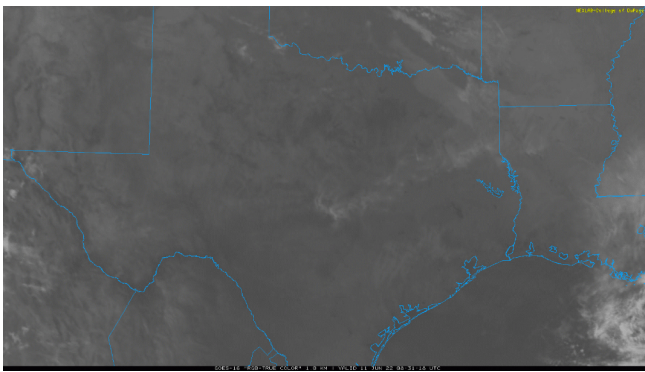


Figure 15. COD nighttime clouds over TX at 0926 UTC 11 June 2022. The COD uses infrared data to fill in the nighttime portions of their images. The low clouds are close to the temperature of the ground, so they are hard to see. [[Click on image for animation.](#)]

the difference between the square of the red brightness and the square of the blue brightness for a dark lava region in northern Mexico.

For beginning pilots, clouds are very important. Fog, broken clouds, or overcast clouds with bases below 304.8 m (1000 ft) will prevent beginning pilots from flying. Satellite images provide a real-time overview of the current cloud locations. Student pilots generally do not have enough satellite image interpretation experience to distinguish high clouds from low clouds. To distinguish high clouds from low clouds, the ERAU day/night visible product tints the high clouds cyan. During the day, channel 4 is used to

make a mask of the location of high cirrus clouds. Within the mask, the brightness of the red (channel 2) is reduced by 15% while leaving the blue and green channels unaffected; this results in the cyan blue color of the high clouds.

During winter over the northern United States, it is difficult to identify clouds and fog over snow during the day. Because the identification of low clouds and fog is important to the aviation industry, the ERAU day/night visible images display snow as a light-yellow color. The *GOES* channel 5 is sensitive to ice particles. Subtracting channel 5 from channel 3 shows snow on the ground and cirrus ice clouds. Channel 4 is sensitive to cirrus clouds during the day. Subtracting channel 4 from the channel 3–5 difference will eliminate the cirrus clouds, leaving only the snow on the ground. To merge the snow image into the color visible, 35% of the brightness of the snow image is subtracted from the blue image. By subtracting values from the blue, the remaining red and green will generate a yellow color for the areas with snow on the ground. For the stand-alone snow product, there are some false alarms caused by low glaciated clouds that are over bare ground. However, these false-alarm clouds in the snow image are generally quite dim while the snow is quite bright. The 35% reduction in brightness of the snow image in the ERAU product makes the dim false-alarm clouds even dimmer. The net effect is that one does not see the potential false alarms. At night, the low-cloud algorithm does not identify snow on the ground, so the yellow snow disappears. Also, as the snow is melting, it loses its crystalline structure and the yellow snow reverts to white. Figure 16 shows an example of snow on the ground, high clouds, and low clouds using the original *GOES* channel 2 visible. Figure 17 shows the same scene with the snow tinted yellow, the cirrus clouds tinted blue, and the low clouds as white.

The advantages of a colored background allowing users to distinguish dim clouds more easily from ground described in section 3 is still a valid concern at night. The ERAU day/night color visible algorithm attempts to generate a nighttime synthetic image that looks as close as possible to the daytime color visible image. The low-clouds image is generated using the method of Ellrod (1995) by computing the brightness temperature difference between channels 13 and 7 and stretching the result into the entire brightness range of the display (e.g., a temperature difference of -6 to $+5^{\circ}\text{C}$ is stretched into 0 to 255 counts). For high clouds, the algorithm uses the brightness temperature difference

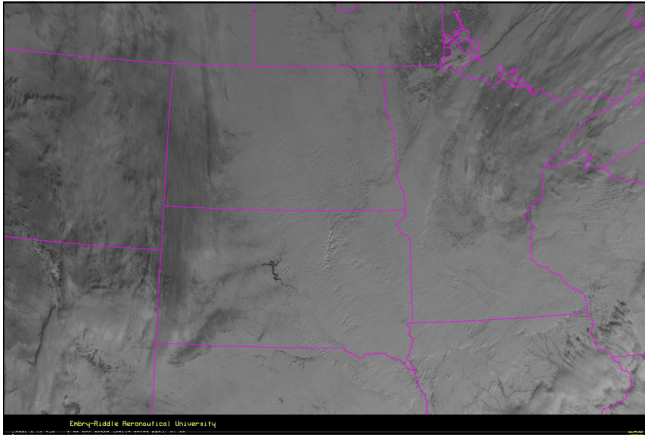


Figure 16. GOES visible (channel 2) image over the Dakotas at 1651 UTC 30 December 2020. It is difficult to distinguish among the snow on the ground, high clouds, and low clouds.

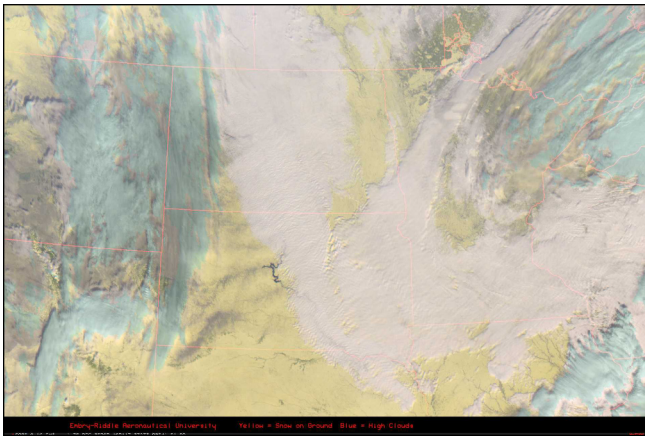


Figure 17. ERAU day/night image for the same time and location as in Fig. 16. The high cirrus clouds have been identified using GOES channel 4 and tinted blue. The snow has been identified using channels 4 and 5 subtracted from channel 3 and tinted yellow. The low clouds are white.

between the channel 12 ozone band and the channel 13 clear-window band (i.e., channel 12–channel 13 temperature difference of -25 to $+25^{\circ}\text{C}$ stretched between brightness counts of 60 to 255). There is an emissivity difference in high clouds between the two channels that is dependent on cloud thickness. This allows one to see the cloud top texture and the difference between cirrus and thunderstorm clouds, like the daytime visible reflectance that also depends upon cloud thickness.

To generate nighttime color images, three component images are needed: a red, blue, and green

image. The high-cloud/low-cloud composite described above can be utilized as the red image and can be used as a starting point for the blue and green images. To generate the nighttime blue image, a land/sea mask is used to determine pixels that are over water. Both channels 13 (clear infrared) and 16 (CO_2) are corrected for limb darkening, and then the difference between the two channels is used to determine clear pixels. A difference threshold of 20 counts (10K) or greater is used to define clear pixels. For clear pixels over water, the nighttime red and green channels have the clear brightness decreased by 50%, and the nighttime blue channel decreased by 25%. This gives the clear pixels a dark blue color. Over land, the variable emissivity of the surface makes the channel 13–16 difference unreliable for the determination of clear pixels. For land pixels in the green image, a threshold clear-sky value (85 counts) is defined, and a bump up count is added to the nighttime clear pixels. The green bump up value for each pixel is computed from the difference between the red and green daytime cloud-free images. The cloud-free images are generated using a month-long minimum brightness composite of the satellite noon images. This method allows for seasonal changes in greenness.

The insertion of color into the clear-sky nighttime images depends on a threshold clear-sky brightness value. No threshold brightness is perfect in delineating cloud/no cloud. Some small clouds with brightness values below the threshold can be misidentified as land or sea and colored inappropriately.

Figure 18 shows the ERAU day/night visible color GOES-East image at 1251 UTC 14 May 2021 (the same time as in Figs. 11, 12, and 14). The high clouds have been tinted blue, while the low clouds are white. The snow on the mountains of British Columbia and Alberta is tinted yellow. The image has been remapped into a Lambert Conformal projection. Areas not scanned by the 5-min CONUS scan (bottom left corner of image) have been filled in with 10-min full-disk scan data. Figure 19 shows ERAU nighttime clouds over Texas with low clouds being white and high clouds being cyan.

8. CIRA/NOAA GeoColor imagery

GeoColor is an application developed by CIRA at CSU that aims to consolidate disparate information and facilitate scene interpretation by the human analyst of geostationary satellite imagery. The GeoColor product (Miller et al. 2020), currently distributed by NOAA,

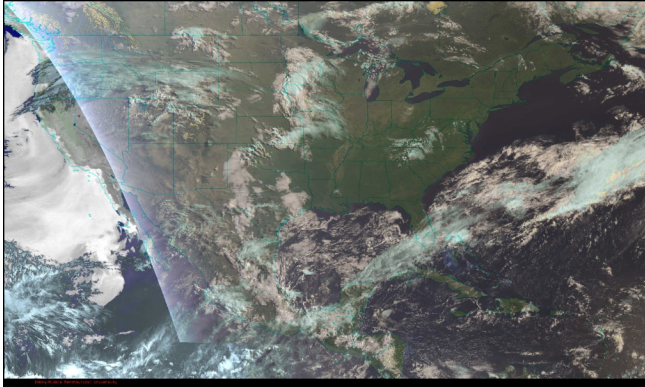


Figure 18. ERAU day/night visible color *GOES-East* image at 1251 UTC 14 May 2021 (the same time as in Figs. 11, 12, and 14). The section of the image to the right of the sunrise diagonal line is derived from visible channels 1 through 5, while the nighttime West Coast section is derived from infrared channels 7, 12, 13 and 16. The high clouds have been tinted blue, while the low clouds are white. Snow on the mountains of British Columbia and Alberta has been tinted yellow (as seen in the animation). The image has been remapped into a Lambert Conformal projection. Areas not scanned by the 5-min CONUS scan (bottom left corner of the image) have been filled in with 10-min full-disk scan data. [Click on image for animation.]

was developed by scientists at CIRA, located at CSU in Fort Collins, Colorado. The ~15-year development effort that culminated in GeoColor included collaboration between CIMSS, the Naval Research Laboratory in Monterey, California, members of the NOAA/NESDIS Regional and Mesoscale Meteorology Branch, and the Advanced Satellite Products Branch, all of whom share credit in developing the final capability. Access to GeoColor data (<https://www.star.nesdis.noaa.gov/GOES>) also includes all 16 channels of the ABI in addition to GeoColor and other multispectral imagery products. The products are available for full-disk, CONUS, 20 *GOES-East* regional sectors, 11 *GOES-West* sectors, and the four floater meso-sectors from *GOES-East* and *GOES-West*—all of which auto-refresh. CSU has an innovative website that features GeoColor and other multispectral imagery applications (<https://rammb-slider.cira.colostate.edu>; Micke 2018). The Naval Research Laboratory (NRL) hosts similar imagery on their NexSat website (Miller et al. 2006; <https://www.nrlmry.navy.mil/NEXSAT.html>). While the user interfaces at CSU and NRL are unique and innovative, the GeoColor product is the same as that

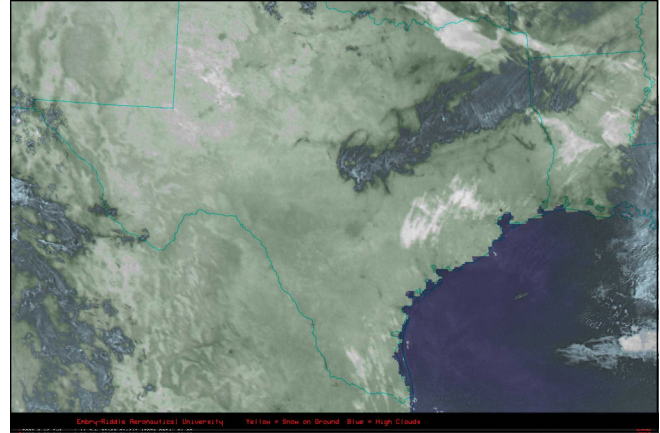


Figure 19. ERAU nighttime clouds over TX at 0926 UTC 11 June 2022. Low clouds are white, high clouds are cyan, land is shades of green, and water is dark blue. [Click on image for animation.]

being hosted on the NOAA website. GeoColor images typically are displayed in the native satellite projection. NWS forecasters can access the GeoColor data on their AWIPS workstations by accessing the data via a Local Data Management feed rather than the conventional NOAAPort feed utilized by the other GOES satellite products.

The CIRA/NOAA method described in section 3 for the generation of a synthetic green channel has the side benefit of performing a brightness normalization for all three channels. The use of the Rayleigh scattering correction for all three channels and the nonlinear synthetic green channel results in the CIRA/NOAA color palette being more vibrant than the colors seen in other color visible image products.

Nighttime GeoColor imagery attempts to mimic what a human observer on the satellite would see during a nighttime moonlit view of the Earth by a low-light visible sensor [e.g., the VIIRS Day/Night Band (DNB); Miller et al. 2013], but additionally includes some false-color components. The nighttime low-cloud image is generated similarly to the ERAU low-cloud image, using the brightness temperature difference between channel 7 and channel 13, leveraging the cloud-top particle-size emissivity sensitivity of low clouds to distinguish them from the surface and any higher-level clouds. The GeoColor low clouds are given a blue tint to distinguish them from high clouds. GeoColor nighttime high clouds are generated from ABI channel 13, like the COD nighttime clouds. Thresholds are utilized to distinguish between cloudy

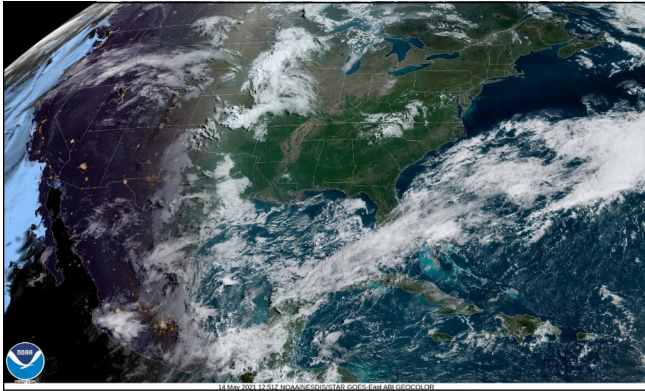


Figure 20. CIRA/NOAA GeoColor image at 1251 UTC 14 May 2021 (the same time as in Figs. 11, 12, 14, and 18). The nighttime portion of the image (West Coast) shows high clouds as white, low clouds as blue, and city lights and terrain in clear areas. East of the sunrise line (from western WA to southern CA), the nighttime and daytime images have been blended to provide a gradual transition between day and night. The image is shown in the original *GOES* projection. [[Click on image for animation.](#)]

and clear areas in the GeoColor low- and high-cloud imagery layers. For the low-cloud night layer, the minimum threshold value is slightly higher over land than water to prevent some forms of terrain from being misidentified as clouds. As with any threshold technique, some small clouds can be misinterpreted as clear sky.

A static image of nighttime city lights, combined with a terrain background, serves as the base layer of GeoColor. The locations of the nighttime city lights come from the polar-orbiting Suomi National Polar-orbiting Partnership VIIRS DNB 2015 annual composite (Hillger et al. 2013), remapped into the *GOES* projection. A yellow/orange color is utilized to simulate sodium street lighting. In clear areas outside the range of city lights, an elevation database is used to impart a nocturnal deep blue/purple image of surface terrain. Both the low- and high-cloud layers of GeoColor employ a variable transparency that is dependent on either the magnitude of the low-cloud signal or the temperature of the cloud top. This allows the city lights to “shine through” the meteorological clouds. This transparency operates at the pixel level, and there is no attempt to diffuse the upwelling city light as is observed via actual DNB imagery. Nonetheless, the city lights provide users with an

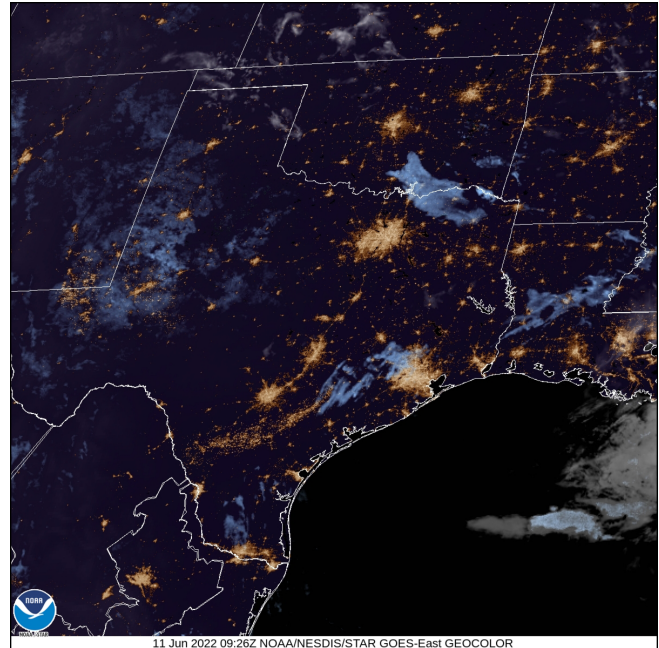


Figure 21. CIRA/NOAA nighttime clouds over TX at 0926 UTC 11 June 2022. The low clouds are blue, the high clouds are gray, the city lights are orange, and clear areas are black. [[Click on image for animation.](#)]

additional sense of orientation beyond traditional displays of state/political boundaries and latitude/longitude grids.

The COD and ERAU products have an abrupt transition between daytime and nighttime imagery within the sunrise/sunset terminator zone. By contrast, the GeoColor product utilizes a gradual blending of the daytime and nighttime images. Starting at the terminator zone and extending 15° of solar zenith angle into the daylight portion of the image (approximately one hour of daylight), the nighttime image is gradually blended with the daytime image. Figure 20 shows the CIRA/NOAA GeoColor image at 1251 UTC 14 May 2021. The nighttime portion of the image (West Coast) shows high clouds as white, low clouds as blue, and city lights and terrain in the clear areas. East of the sunrise line (from eastern Montana to southern California) the nighttime and daytime images have been blended to provide a gradual transition between day and night. Figure 21 shows GeoColor nighttime clouds over Texas.

9. Summary and conclusions

The human eye has sensors for three different wavelengths of light within red, green, and blue

Table 1. The attributes of the producers discussed in this paper. C represents a *GOES* channel (e.g., C1 is channel 1, which is the blue channel on *GOES*).

Attributes	SSEC	COD	ERAU	CSU/NOAA	CSPP/GeoSphere
Synthetic Green	Linear .45(C1)+.45(C2)+ .10(C3)	Linear .45(C1)+.45(C2)+ .10(C3)	Linear .36(C1)+.40(C2)+ .20(C3)	Nonlinear Lookup Table	Linear .465(C1)+.465(C2) +.07(C3)
Projection	Satellite	Remapped	Remapped	Satellite	Satellite
Rayleigh Correction	None	C1 (blue) Correction	C1 (blue) Correction	C1, C2, C3 corrections	C1, C2, C3 corrections
Brightness Normalization	None	Yes	Yes	Yes	Yes
Daytime Low Clouds	White	White	White	White	White
Daytime High Clouds	White	White	Cyan	White	White
Nighttime Low Clouds	None	C7 White	C13-C7 White	C13-C7 Blue	Blue to Yellow
Nighttime High Clouds	None	C7 White	C13-C12 Cyan	C13 White	C15-C13 Red to Black
City Lights	None	None	None	Nighttime	None
Day/Night Transition	Fade to Black	Abrupt Transition at Sunrise/ Sunset	Abrupt Transition at Sunrise/Sunset	1-h Gradual Transition	10-min Gradual Transition
Snow on Ground (daytime)	White	White	Yellow	White	White

wavelengths. The human eye is not very sensitive to variations in shades of gray—being able to distinguish only approximately 25 different gray shades in satellite images. By using the three-color sensors, the eye has the potential to distinguish up to a million different values of color. Hence, color is a powerful tool for distinguishing various objects of interest with subtle intensity variations.

In planning the *GOES-R* series of geostationary satellites, NOAA did not have a formal requirement for color images, so *GOES-16* was launched with red, blue, and near-infrared channels—but no green channel. The near-infrared veggie channel responds strongly to sunlight reflected by vegetation. While reflected light from vegetation is about five times as strong as the green seen by the human eye, the cloud reflectance is about the same in the veggie channel as in the red and blue channels. A synthetic green channel can be generated using a combination of the red, blue, and veggie channels.

Since the launch of the *GOES-16* satellite, five different groups have developed color visible algorithms that are available on public websites (as previously noted). Because there is no formal government requirement for a color visible image product, the different groups were free to develop what they consider an appropriate color visible product. The attributes of the various methods are summarized in Table 1.

In addition to the websites described in this paper, there are several spinoff sites that contain color visible images. The Brazil Government weather website (<https://www.cptec.inpe.br/dsat>) has a product like the CSPP, except at night the Brazilians use an infrared image instead of the nighttime image. The Government of Chile (<http://www.meteochile.gob.cl/PortalDMC-web/index.xhtml>) has color visible images like SSEC. The Government of Mexico (<http://www.lanot.unam.mx/goes.php>) has a daytime color visible image product like CIRA/NOAA but with a colorized infrared image at night that includes nighttime city lights. Within the

United States, the National Center for Atmospheric Research/Research Applications Laboratory has a website (<https://weather.rap.ucar.edu/satellite/>) that contains a color visible like the basic SSEC product that gets dark at night. The University of Hawaii has a website (<http://weather.hawaii.edu/>) that offers a true-color image based on the SSEC technique. The University of Washington has a website (<https://a.atmos.washington.edu/data/>) that contains a color visible selection like the one at COD with color visible during the day and gray-scale infrared at night. AccuWeather has a satellite color visible product (<https://www.accuweather.com/en/us/national/satellite>) that is very similar to the CIRA/NOAA product, although the colors are not as vivid. As mentioned in section 8, CSU and NRL feature the CIRA/NOAA GeoColor.

The above list of websites—each featuring some version of a true-color visible satellite image—shows that there is a demand for this type of product. At many of these websites the true-color visible is the first choice available for users to select. A suggested future study would be to look at the number of user requests for true-color visible as compared to other possible satellite image selections. NOAA should consider adding a true green channel to the next generation of geostationary weather satellites.

Within the five featured websites, the daytime truecolor visible products are reasonably similar. However, there is a large difference in the nighttime imagery. Another suggested future study would be to poll users in various sectors on their nighttime information requirements.

Acknowledgments. Much of the image processing described in this article was done using the McIDAS-X software package available from the McIDAS Users Group, administered by the SSEC at the University of Wisconsin-Madison. Mat Gunshor, CIMSS, is thanked for Fig. 3. Chris Schmidt, CIMSS, is thanked for his early work on generating true-color imagery. The views, opinions, and findings contained in this report are those of the authors and should not be construed as an official NOAA or United States government position, policy, or decision.

REFERENCES

- Bah, M. K., M. M. Gunshor, and T. J. Schmit, 2018: Generation of *GOES-16* true color imagery without a green band. *Earth Space Sci.*, **5**, 549–558, [Crossref](#).
- Corbell, R. P., C. J. Callahan, and W. J. Kotsch, 1976: The *GOES/SMS* User's Guide. NOAA National Environmental Satellite Service, Suitland, MD, 126 pp. [Available online at https://docserv01.gesdisc.eosdis.nasa.gov/repository/Mission/Nimbus/3.3_Product_Documentation/3.3.5_Product_Quality/GOES_SMS_Users_Guide.pdf.]
- Davis, G. K., 2001: *GOES* Users' Conference: Conference Report. U.S. DOC/NOAA/NESDIS, Broomfield, CO, 45 pp. [Available online at https://www.goes-r.gov/downloads/users/conferencesAndEvents/2001/GUC_Report.pdf.]
- _____, 2004: 3rd *GOES-R* Users Conference: Conference Report. U.S. DOC/NOAA/NESDIS, Broomfield, CO, 97 pp. [Available online at <https://www.goes-r.gov/downloads/users/conferencesAndEvents/2004/GUC/GUC3ConferenceReport.pdf>.]
- Ellrod, G. P., 1995: Advances in the detection and analysis of fog at night using *GOES* multispectral infrared imagery. *Wea. Forecasting*, **10**, 606–619, [Crossref](#).
- Goodman, S. J., and Coauthors, 2012: The *GOES-R* Proving Ground: Accelerating user readiness for the next-generation geostationary environmental satellite system. *Bull. Amer. Meteor. Soc.*, **93**, 1029–1040, [Crossref](#).
- Hillger, D., and Coauthors, 2013: First-light imagery from Suomi NPP VIIRS. *Bull. Amer. Meteor. Soc.*, **94**, 1019–1029, [Crossref](#).
- Hunt R. W. G., 2004: *The Reproduction of Colour*. 6th ed., John Wiley & Sons, 724 pp.
- McQuain, R. H., 1967: ATS-I camera experiment successful. *Bull. Amer. Meteor. Soc.*, **48**, 74–79, [Crossref](#).
- Micke, K., 2018: Every pixel of *GOES-17* imagery at your fingertips. *Bull. Amer. Meteor. Soc.*, **99**, 2217–2219, [Crossref](#).
- Miller, S. D., and Coauthors, 2006: NexSat: Previewing NPOESS/VIIRS imagery capabilities. *Bull. Amer. Meteor. Soc.*, **87**, 433–446, [Crossref](#).
- _____, C. C. Schmidt, T. J. Schmit, and D. W. Hillger, 2012: A case for natural colour imagery from geostationary satellites, and an approximation for the *GOES-R* ABI. *Int. J. Remote Sens.*, **33**, 3999–4028, [Crossref](#).
- _____, 2013: Illuminating the capabilities of the Suomi National Polar-orbiting Partnership (NPP) Visible Infrared Imaging Radiometer Suite (VIIRS) Day/Night Band. *Remote Sens.*, **5**, 6717–6766; [Crossref](#).

- _____, T. L. Schmit, C. J. Seaman, D. T. Lindsey, M. M. Gunshor, R. A. Kohrs, Y. Sumida, and D. Hillger, 2016: A sight for sore eyes: The return of true color to geostationary satellites. *Bull. Amer. Meteor. Soc.*, **97**, 1803–1816, [Crossref](#).
- _____, D. T. Lindsey, C. J. Seaman, and J. E. Solbrig, 2020: GeoColor: A blending technique for satellite imagery. *J. Atmos. Oceanic Technol.*, **37**, 429–448, [Crossref](#).
- Schmit, T. J., M. M. Gunshor, W. P. Menzel, J. J. Gurka, J. Li, and A. S. Bachmeier, 2005: Introducing the next-generation Advanced Baseline Imager for *GOES-R*. *Bull. Amer. Meteor. Soc.*, **86**, 1079–1096, [Crossref](#).
- _____, P. Griffith, M. M. Gunshor, J. M. Daniels, S. J. Goodman, and W. J. Lebar, 2017: A closer look at the ABI on the *GOES-R* series. *Bull. Amer. Meteor. Soc.*, **98**, 681–698, [Crossref](#).
- _____, S. S. Lindstrom, J. J. Gerth, and M. M. Gunshor, 2018: Applications of the 16 spectral bands on the Advanced Baseline Imager (ABI). *J. Operational Meteor.*, **6** (4), 33–46, [Crossref](#).
- Suomi, V. E., and R. J. Parent, 1968: A color view of planet Earth. *Bull. Amer. Meteor. Soc.*, **49**, 74–75, [Crossref](#).
- _____, R. Fox, S. S. Limaye, and W. L. Smith, 1983: McIDAS III: A modern interactive data access and analysis system. *J. Climate Appl. Meteor.*, **22**, 766–778, [Crossref](#).
- Tucker, C. J., 1979. Red and photographic infrared linear combinations for monitoring vegetation. *Remote Sens. Environ.*, **8**, 127–150, [Crossref](#).
- Warnecke, G., and W. S. Sunderlin, 1968: The first color picture of the Earth taken from the *ATS-3* satellite. *Bull. Amer. Meteor. Soc.*, **49**, 75–83, [Crossref](#).